Microwave pump-probe spectroscopy of the dipole-dipole interaction in a cold Rydberg gas

Hyunwook Park, T. F. Gallagher, and P. Pillet

Phys. Rev. A **93**, 052501 — Published 2 May 2016

DOI: 10.1103/PhysRevA.93.052501

Microwave pump-probe spectroscopy of the dipole-dipole interaction in a cold Rydberg gas

Hyunwook Park*
Department of Physics, The Ohio State University, Columbus, Ohio 43210, USA.

T. F. Gallagher
Department of Physics, University of Virginia, Charlottesville, Virginia 22904-0714, USA.

P. Pillet
Laboratoire Aimé Cotton, CNRS, Univ. Paris-Sud, ENS Cachan, Bât. 505, 91405 Orsay, France.

Microwave pump-probe experiments starting from a cold gas of Rb $34s$ atoms confirm that cusped lineshapes observed in dipole-dipole broadened microwave transitions are due to atoms which are widely separated and exhibit small dipole-dipole energy shifts. When the experiments are interpreted in terms of a nearest neighbor model, they demonstrate that it is possible to select pairs of atoms based on their separation and orientation.

I. INTRODUCTION

Microwaves have proven to be a useful tool for the study and manipulation of cold Rydberg atoms. Examples of the latter are the use of AC Stark shifts for tuning, the initiation of ionization by transferring pairs of atoms to attractive dipole-dipole potentials and the observation of the dipole-dipole interactions of microwave dressed atoms [1–5]. Examples of the former are monitoring the motion of pairs of atoms on repulsive van der Waals potentials and measurements of dipole-dipole line broadening [6, 7]. Unlike classic collisional line broadening measurements, the dipole-dipole broadening leads to distinctly cusp shaped lines. A striking example is shown in Fig. 1. The cusped shape has been attributed to pairs of atoms which have small or vanishing dipole-dipole energy shifts [7]. Atoms which are far apart always have small shifts, and the inhomogeneous density distribution of our cold atom sample leads to the cusped lineshape [7]. There are also cases in which pairs with small spacing, R, have zero dipole-dipole shifts. These states are analogous to the "Förster zero" pair states which have vanishing van der Waals shifts [8].

Here we report the investigation of the dipole-dipole interactions of cold Rb Rydberg atoms using microwave pump-probe spectroscopy. Specifically, using a pump microwave pulse at or near the $34s_{1/2} - 33p_{3/2}$ atomic frequency we depopulate the $34s_{1/2}34s_{1/2}$ state, and we observe the pump's effect using the probe pulse, which is scanned across the atomic $34s_{1/2} - 34p_{1/2}$ resonance frequency. When the pump pulse is tuned to the atomic $34s_{1/2} - 33p_{3/2}$ frequency, relatively isolated atoms, those with large R, are removed from the sample of $34s_{1/2}34s_{1/2}$ pairs, and the cusp in the lineshape observed with the probe pulse disappears, consistent with the explanation for its existence [7]. When the pump pulse is detuned from the atomic $34s_{1/2} - 33p_{3/2}$ transition frequency the resulting asymmetric lineshapes observed with the probe pulse show that the pump pulse has transferred $34s_{1/2}34s_{1/2}$ pairs with selected R and orientation to the $34s_{1/2}33p_{3/2}$ state. The microwave transitions driven by the pump pulse are transitions which produce entangled pairs of atoms, just as in microwave transitions in which both atoms change state and Förster resonant energy exchange [9–12]. In the sections which follow we present a nearest neighbor model, outline the basic concept of the experiment, summarize the essential features of the approach, present our observations, and discuss their implications.

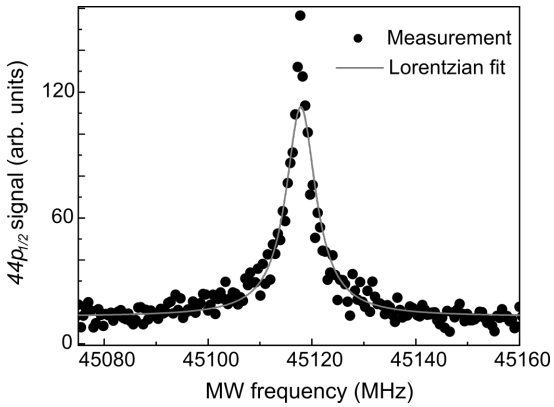

FIG. 1. A typical cusp spectrum observed in $ns_{1/2}ns_{1/2} - ns_{1/2}np_{1/2}$ microwave transitions from a high density Rydberg sample. This example is from $n = 44$ with the peak atomic density of $\rho_0 = 1.3 \times 10^9 \mathrm{cm}^{-3}$. Experimental points (•), and Lorentzian fit (solid line).

II. NEAREST NEIGHBOR MODEL OF THE FROZEN RYDBERG GAS

To interpret our observations we make two assumptions. First, we assume the atoms to be frozen in place. Second, we assume that only binary interactions are important. At a temperature of 300 μK the average speed of a Rb atom is 20 cm/s. The time scale of the experiment is 2 μs, during which time the atoms move 2%

* park.1771@osu.edu

of their average spacing at a density of 10^9 cm^{-3}. The conditions of the first assumption are well met.

In a regular array of atoms the second approximation would be terrible, but in our sample the atoms are randomly located, which has two implications. First, in such samples dipole-dipole line broadening is dominated by pairs of atoms which are close to each other [13]. In early measurements of Stark tuned resonant dipole-dipole energy transfer in the frozen Rydberg gas the widths of the resonances were observed to be an order of magnitude larger than the dipole-dipole interaction of two atoms the average spacing apart [11, 12]. These pairwise interactions between nearest neighbors are estimated to account for approximately two thirds of the observed widths [13]. In a later experiment an "always resonant" interaction twelve times as strong as the one tuned into resonance was added, but it only broadened the resonance by a factor of three [14], which is consistent with the calculations [13]. In sum, by assuming that the observed spectral broadening is due only to binary interactions between pairs of close atoms we are ignoring one third of the dipole-dipole interactions. Although we expect this model to capture the essential physics, it has its shortcomings.

The second effect of the random locations of the atoms is to mask any macroscopic coherence. The random distances between atoms introduces randomness in the strengths of the dipole-dipole interactions, and the random orientations of the microwave field, relative to the internuclear axes, as shown in Fig. 2b, introduces randomness into the strength of the microwave coupling.

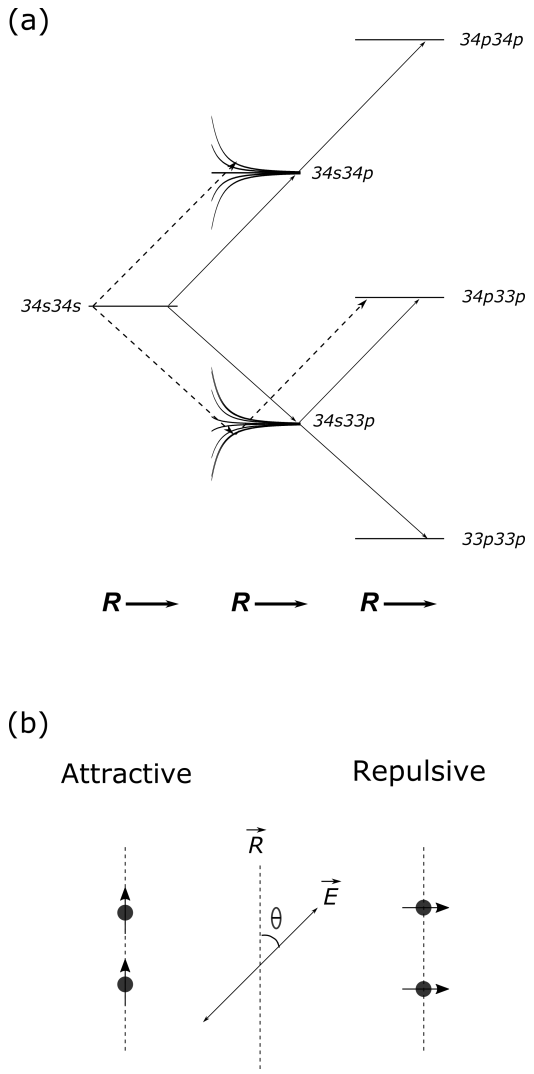

FIG. 2. (a)Schematic energy level diagram showing the relevant molecular energy levels as a function of internuclear spacing R. The internuclear axis is taken to be the axis of quantization. The solid downward arrows show the transitions driven from the initially populated $34s34s$ state by an on resonant pump pulse, and the broken downward arrows show the transition driven by an off resonant pump pulse. The solid upward arrows show the transitions driven by an on resonant probe pulse, and the broken upward arrows show the transitions driven by an off resonant probe pulse. (b)Classical picture of the interacting atomic dipoles. The broken vertical line is the internuclear axis. In the attractive states the two atomic dipoles are parallel to the internuclear axis, and in the repulsive states the dipoles are perpendicular to the internuclear axis. The microwave field E is randomly oriented relative to the internuclear axis.

III. PRINCIPLE OF THE EXPERIMENT

The principle of the experiment is easily understood with the help of Fig. 2a, an energy level diagram of the relevant molecular states. Fig. 2a shows the diatomic energy levels using the internuclear axis as the quantization axis. Fig. 2b is a more intuitive classical picture suggesting the origin of the energy levels of Fig. 2a. In the attractive dipole-dipole states the atoms have their dipole moments parallel to the inrternuclear axis, and in the repulsive states the atomic dipoles are perpendicular to the internuclear axis. Fig. 2b also brings out the important point that the microwave polarization is randomly oriented relative to the internuclear axis of any pair of atoms.

The molecular states are direct products of the atomic $34s_{1/2}, 34p_{1/2}$, and $33p_{3/2}$ states. For simplicity of notation we shall refer to these atomic states as the $34s$, $34p$, and $33p$ states. A typical molecular state is $34s34p$. There are many $34s34p$ and $34s33p$ states, as shown in Fig. 2a, due to the inclusion of the Rydberg electrons' spin. One of the essential points shown in Fig. 2a is that the $34s34p$ and $34s33p$ states exhibit large dipole-dipole energy shifts, but the $34s34s$, $34p34p$, $33p34p$, and $33p33p$ states exhibit only van der Waals shifts, which are insignificant in this context [15]. We have chosen to use the $33p_{3/2}$ level instead of the $33p_{1/2}$ level because it does not lead to a $34s33p$ level with no dipole-dipole energy shift, i. e., there is no Förster zero state [7, 8].

Using pulsed laser excitation of cold Rb atoms in a magneto-optical trap (MOT) we produce the $34s34s$ state of Fig. 2a. Laser excitation is immediately, in 50 ns, followed by the microwave pump pulse which is 1 μs long and fixed in frequency, at or very near the atomic

$34s-33p$ frequency of 117.1 GHz. We consider first the effects of on and off resonant pump pulses. When the pump pulse is on resonant, i.e. tuned to the atomic frequency, it drives $34s34s$ pairs with large R to the $34s33p$ and $33p33p$ states, as shown by the solid downward arrows of Fig. 2a. To be precise, it drives pairs with R large enough that the dipole-dipole shift is smaller than the $34s-33p$ Rabi frequency. If the microwave pump pulse is off resonant, it drives pairs with relatively small R and the appropriate orientation of their internuclear axes relative to the linearly polarized microwave pump field to the $34s33p$ state. To drive the pump transition to the attractive (repulsive) $34s33p$ state the internuclear axis must be parallel (perpendicular) to the microwave field. In Fig. 2a we show by the broken downward arrow the transition driven by a pump pulse tuned to a frequency slightly higher than the $34s-33p$ atomic frequency. Both on resonant and off resonant pump pulses deplete the population in the $34s34s$ state.

We now consider the effect of the probe pulse. The probe pulse, also 1 μs long, is applied 200 ns after the end of the pump pulse. It is scanned in frequency through the atomic $34s-34p$ frequency, and we detect atoms in the $34p$ state by field ionization. Atoms are left in the $34p$ state, and can be detected, as a result of the molecular transitions shown by the upward arrows of Fig. 2a. At the atomic transition frequency the probe pulse drives $34s34s$ pairs with large R to both the $34s34p$ and $34p34p$ states, as shown by the solid upward arrows from the $34s34s$ state in Fig. 2a. It is worth noting that field ionization of the $34p34p$ state yields twice the $34p$ field ionization signal of the $34s34p$ state, which also contributes to the cusp. Away from the atomic resonance frequency the probe pulse drives $34s34s$ pairs with relatively small R and the appropriate orientation of their internuclear axes relative to the linearly polarized microwave probe field to the $34s34p$ state, as shown by the broken upward arrow from the $34s34s$ state. To drive the probe transition to the attractive (repulsive) $34s34p$ state the internuclear axis must be parallel (perpendicular) to the microwave probe field, which is parallel to the pump field. The probe pulse can also drive transitions to the $34p33p$ state from $34s33p$ pairs with both large and small R, as shown by the solid and broken upward arrows, respectively.

IV. EXPERIMENTAL APPROACH

Since the experimental apparatus and the essence of the approach have been described in some detail elsewhere, our description here is brief [7, 15]. Cold ^{85}Rb atoms are held in a vapor loaded MOT, and Rb atoms are excited to the $34s$ state by a 10 ns long 480 nm pulse at a 20 Hz repetition rate. The 480 nm pulse is generated by frequency doubling the pulse-amplified output of a single mode 960 nm diode laser. The density in the MOT is a Gaussian with a radius r_M=45 μm, and the 480 nm laser beam propagates in the z direction and is focused to a waist of radius r_L=160 μm.

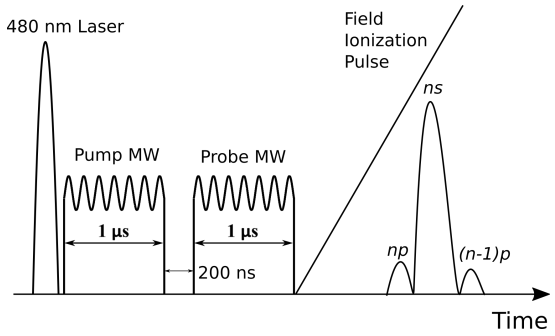

FIG. 3. Timing diagram of the experiment, showing laser excitation, pump and probe field microwave pulses, field ionization pulse and field ionization signals.

As a result, the density of Rydberg atoms is given by $\rho(x,y,z)=\rho_0 e^{-z^2/r_M^2} e^{-(x^2+y^2)}/r_L^2$, where ρ_0 is the density of Rydberg atoms at the center of the MOT. In these experiments $\rho_0 = 1.7\times10^9 \mathrm{cm}^{-3}$, and at this density the full width at half maximum of the dipole-dipole broadened $34s34s-34s34p$ transitions is 4 MHz.

The timing sequence for the experiment, starting with the pulsed laser excitation, is shown in Fig. 3. Not shown is the fact that the MOT magnetic fields are switched off 6 ms before the laser fires, so that the magnetic field is reduced to an insignificant level, $\leq$50 mG, when the laser fires. As shown in Fig. 3, immediately after laser excitation the 1 μs microwave pump pulse at frequency 117.1 GHz is used to drive the $34s34s-34s33p$ transition. The frequency is either fixed at the atomic $34s-33p_{3/2}$ frequency of 117.1 GHz, so as to excite only atoms which are far from each other, or the frequency is detuned from the atomic frequency, to drive transitions of $34s34s$ pairs with smaller R to the $34s33p$ state. After a 200 ns delay the 1 μs long microwave probe pulse is applied, to drive the $34s34s-34s34p$ transition. Approximately 50 ns after the probe pulse an ionizing field pulse with an amplitude of 1.2 kV/cm and a 2 μs rise time is applied to the atoms. Atoms in the $34p$ state are ionized earlier in the pulse and are easily distinguished from $34s$ atoms. Atoms in the $33p$ state are ionized only slightly after the $34s$ state and are not so easily distinguished from them. The data displayed here are the $34p$ field ionization signals observed as the frequency of the microwave probe pulse is slowly scanned across the $34s-34p$ resonance frequency over many shots of the laser. We assume that the field ionization pulse projects the two atoms in the pair onto effectively isolated atomic states [16].

The microwave fields are generated by two Agilent 83622B frequency synthesizers. The continuous wave outputs of the synthesizers are formed into 1 μs pulses with switches. The 117.1 GHz pulse for the $34s-33p$ transition goes to a DBS-2640X220 active doubler followed by a Pacific Millimeter W3WO passive tripler and a precision attenuator. The 104.1 GHz pulse for the $34s-34p$ transition goes into an active DBS-4060X410 quadrupler and then to a Pacific Millimeter V2WO passive doubler, followed by an attenuator. Both microwave

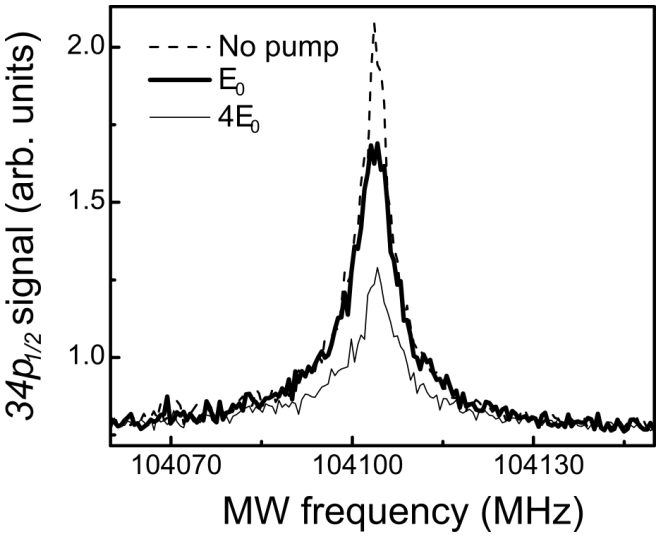

FIG. 4. Observed $34p$ signal as a function of probe frequency for no pump pulse (broken line), pump pulse of amplitude E_0 (bold line), and amplitude $4E_0$ (light line). With pump amplitude E_0 only atoms with large internuclear separations are removed from the $34s34s$ state, and the primary effect is removal of the cusp seen with no pump pulse. With pump amplitude $4E_0$ the entire signal is reduced in size since pairs with smaller internuclear spacings are removed from the $34s34s$ state.

pulses are transported by waveguide to horns just outside a window of the vacuum chamber, and the two microwave pulses propagate through the window into the vacuum system. The microwave field amplitude of the $34s - 34p$ transition is set so as to produce a 2.5 MHz linewidth resonance at low density and is not altered. The amplitude of the 117.1 GHz microwave pulse driving the $34s - 33p$ transition is varied from a low field, at which the Rabi frequency is much less than the dipole-dipole broadening, to a relatively strong field, at which the Rabi frequency is substantially greater than the $34s34s - 34s4p$ dipole-dipole broadening of 4 MHz (FWHM). The linear polarizations of the two microwave fields are parallel.

V. OBSERVATIONS AND DISCUSSION

The dashed trace of Fig. 4 is the $34s34s - 34s34p$ resonance signal obtained when there is no microwave pump pulse to drive the $34s - 33p$ transition. It exhibits dipole-dipole broadening of 4 MHz and a distinctly cusped shape. The solid trace shows the $34s - 34p$ resonance observed when the atoms have been exposed to a resonant $34s - 33p$ pump pulse with microwave field amplitude E_0, which produces a 1 MHz Rabi frequency. The resonant $34s - 33p$ pump pulse removes $34s$ atoms for which the dipole-dipole interactions with neighboring atoms are weak. These atoms could be on the edge of the trap, where all the atoms are far apart, or in the center of the trap but making transitions to $34s34p$ states with small dipole-dipole shifts. In terms of Fig. 2a, pairs of non-interacting atoms undergo transitions to both the $34s33p$ and $33p33p$ states. Many of these pairs are left in the $33p33p$ state, which can not undergo a transition at the $34s - 34p$ atomic frequency. As a result, the cusp in the lineshape is substantially suppressed, leaving a very nearly Lorentzian lineshape, as shown by the bold solid trace in Fig. 4. If we were driving a microwave transition between two levels we would expect to see a Rabi lineshape, which is a Lorentzian with a Rabi frequency dependent modulation. However, we are not observing a single transition. Rather, there are many $34s34s-34s34p$ transitions due to the many $34s34p$ dipole-dipole states, as shown by Fig. 2a, with different Rabi frequencies and dipole-dipole shifts. In addition, the random orientation of the microwave field relative to the internuclear axes, shown in Fig. 2b, introduces more spread into the Rabi frequencies. The presence of different Rabi frequencies for transitions with the same shift suppresses the modulation leading to an approximately Lorentzian line. Exactly what will be observed when averaging over dipole-dipole shifts is not obvious, but the underlying lineshape is essentially Lorentzian.

With progressively larger amplitudes of the $34s - 33p$ pulse pairs of $34s$ atoms with progressively smaller R are driven to the $34s33p$ state and to the $33p33p$ state. Pairs in the latter state can not be driven to the $34s34p$ or $34p34p$ states by the probe pulse. The $34p$ signal obtained by scanning the probe frequency is thus reduced. With a driving field of $4E_0$, shown in Fig. 4 by the light solid line, effectively all pairs, irrespective of internuclear spacing, can be driven to the $34s33p$ state, with the result that the observed $34s34s-34s34p$ lineshape becomes once again cusp shaped. In Fig. 5 we replot the three traces of Fig. 4 normalized to have peak amplitude 1.0 in all three cases and the best Lorentzian fits. As shown, with no pump and a pump of $4E_0$ the lineshape exhibits a cusp, while the lineshape with pump field E_0 is well reproduced by a Lorentzian.

An alternative way to show the progression seen in Fig. 4 is shown in Fig. 6, in which we plot the difference between the $34s34s - 34s34p$ signals with and without $34s34s - 34s33p$ on resonant pump pulses of two different amplitudes. For the driving field E_0 the difference is a narrow peak (bold solid trace of Fig. 4) corresponding to the removal of the cusp in Fig. 4. When the microwave field is increased to $4E_0$, due to the power broadening of the transition, pairs with small values of R can also make the transition to the $34s33p$ state, so the pump pulse no longer removes only widely separated atoms. In this case the effect of the pump pulse is simply to reduce the amplitude of the $34s34s-34s34p$ signal, and the lineshape remains cusped. With a pump pulse detuned from the atomic transition we can address pairs of atoms with finite internuclear separations, having $34s34s - 34s33p$ transitions at frequencies detuned from the atomic frequency. In Fig. 7 we show the results obtained with three tunings of the pump pulse, 0 and $\pm$ 4.8 MHz from the atomic transition frequency. The pump power is similar to that used to obtain the $4E_0$ data shown in Fig. 4.

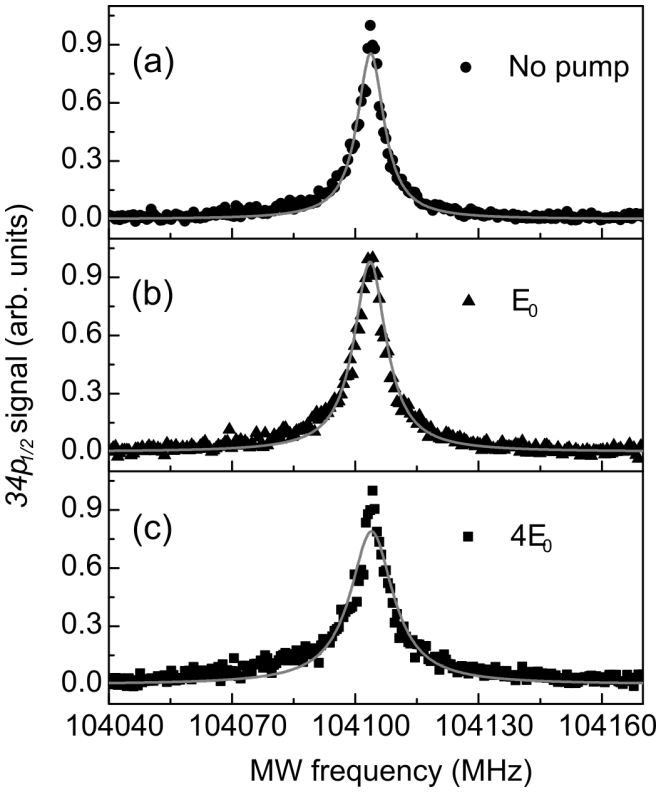

FIG. 5. Observed $34p$ signals of Fig. 4 replotted when normalized to a peak signal of 1.0 in all cases (points) and Lorentzian fits (light lines). In (a), with no pump pulse, there is a cusp on top of the Lorentzian fit. In (b) with pump field E_0 the cusp is removed, and in (c), with pump field $4E_0$ the lineshape is again exhibits a cusp.

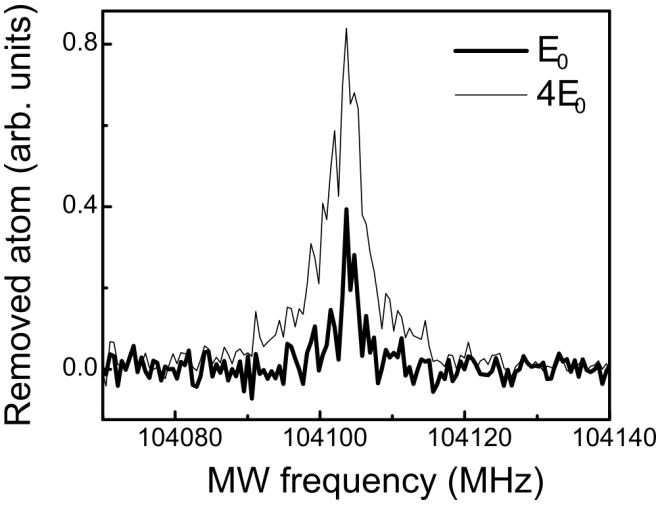

FIG. 6. Difference between the signals obtained with pump amplitude E_0 and no pump pulse (bold line), and difference between the signals obtained with pump amplitude $4E_0$ and no pump pulse (light line). With pump amplitude E_0 only the cusp of the no pump pulse signal is removed, while in the latter case the entire signal is reduced.

As shown in Fig. 7a, if the pump pulse is tuned to the atomic resonance frequency, when the probe frequency is scanned the result is a uniform reduction of the observed $34p$ signal, as expected on the basis of Fig. 4. As shown by Fig. 7b, when the pump pulse is detuned by -4.8 MHz, there is a smaller diminution of the signal than in Fig 7a, and the signal is more depleted on the high frequency side of the atomic resonance than the low frequency side. When the pump pulse is detuned by +4.8 MHz there is again a substantial diminution of the signal relative to no pump pulse. More interesting, the decrease in the signal is now far greater on the low frequency side of the line than on the high frequency side, exactly the opposite of what is observed with a detuning of -4.8 MHz.

The asymmetric lineshapes of Figs. 7b and 7c arise in the following way. For concreteness we consider the lineshape of Fig 7c, obtained with a +4.8 MHz detuning of the pump pulse, but similar reasoning applies to the lineshape of Fig. 7b. As shown in Fig. 2 by the downward broken arrow, the pump pulse drives a close $34s34s$ pair with its internuclear axis parallel to the pump field to an attractive $34s33p$ potential, from which the probe pulse can drive it to the $34p33p$ state. Since the $34p33p$ state has only a small van der Waals energy shift, which is insignificant compared to the dipole-dipole shifts, the $34s33p$ to $34p33p$ transition can only occur if the probe pulse is detuned by approximately +4.8 MHz from the atomic $34s-34p$ frequency, as shown by the upward broken arrow of Fig. 2. In addition, since the pump pulse has removed close $34s34s$ pairs with internuclear axes parallel to the field, there is a preponderance of pairs with internuclear axes perpendicular to the field remaining in the $34s34s$ state. Thus, the probe pulse drives more pairs to the repulsive $34s34p$ state, at a frequency above the atomic $34s-34p$ frequency, than to the attractive $34s34p$ potential, at a frequency below the atomic frequency. More generally, the lineshapes in Figs. 7b and 7c result from two effects of the pump pulse. The first is the removal of close $34s34s$ pairs with a detuning dependent orientation. If the pump pulse drives $34s34s$ pairs to the attractive (repulsive) $34s33p$ state, only pairs with their internuclear axes perpendicular (parallel) to the microwave field are left in the $34s34s$ state, and they are driven to the repulsive (attractive) $34s34p$ state at a frequency above (below) the atomic $34s-34p$ frequency. The second is that the pairs driven to the attractive (repulsive) $34s33p$ potentials can only be driven to the $34p33p$ state by a probe pulse at a frequency above (below) the $34s-34p$ frequency. Both effects of the probe pulse shift the resonance signal observed with the probe pulse in the same direction.

These experiments suggest that, in addition to using a narrow band laser [6, 17], it is possible to select pairs at well defined separations and orientations using microwaves subsequent to pulsed laser excitation. For example, starting from the $34s34s$ state the $34s34p$ state can be prepared on a repulsive or attractive potential curve with a well defined spacing and orientation using an off resonant pump pulse.

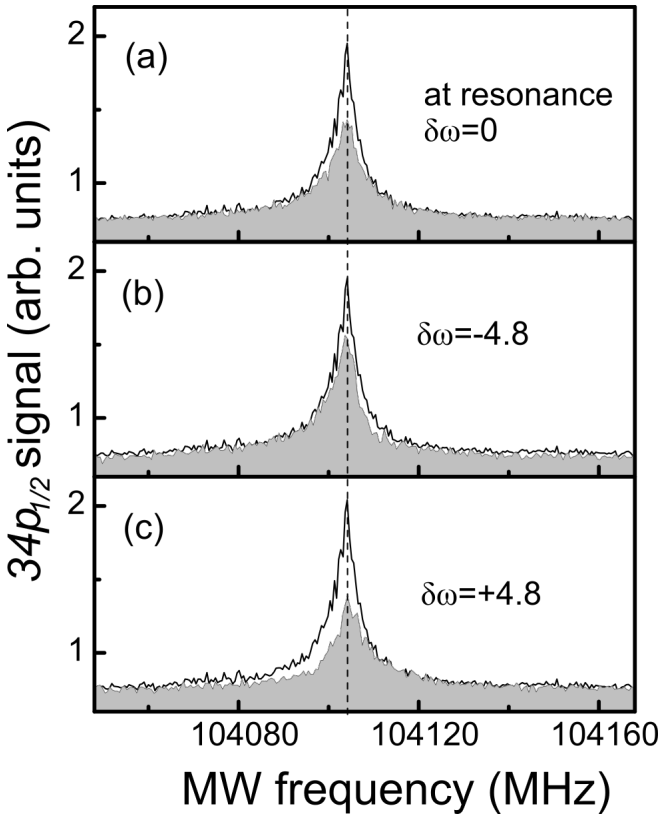

FIG. 7. The effect of on and off resonant pump pulses with amplitude $2E_0$. In all three panels the signals with no pump pulse are shown as solid lines and areas under the signals with the pump pulse are filled. (a) On the $34s - 33p$ resonance the effect is simply an overall diminution of the signal as in the $4E_0$ trace of Fig. 4. (b) With a detuning of -4.8 MHz, there is a larger decrease in the signal above the probe resonance frequency than below it. (c) With a detuning of +4.8 MHz there is a larger decrease in the signal below the probe resonance frequency than above it. The asymmetry in (b) and (c) is due to the fact that off resonant transitions to the $34p33p$ state can be driven, as indicated by Fig. 2a.

VI. CONCLUSION

Using two microwave pulses of different frequencies in a pump-probe arrangement leads to two significant results. First, it shows that the cusp shaped lines observed in dipole-dipole line broadening experiments originate from pairs of atoms which exhibit very small dipole-dipole shifts, as proposed earlier [7]. Second, to the extent that our nearest neighbor model is valid, these experiments show that it is also possible to prepare atoms preferentially at selected interatomic spacings and orientations on attractive or repulsive dipole-dipole potential curves, as has been done with narrow band lasers [6, 17].

ACKNOWLEDGMENTS

This work has been supported by the Air force Office of Scientific Research under grant FA9550-14-1-0288.

[1] P. Bohlouli-Zanjani, J. Petrus, and J. Martin, Physical Review Letters **98**, 203005 (2007).
[2] W. Li, P. J. Tanner, and T. F. Gallagher, Phys. Rev. Lett. **94**, 173001 (2005).
[3] H. Park, E. S. Shuman, and T. F. Gallagher, Phys. Rev. A **84**, 052708 (2011).
[4] E. Brekke, J. O. Day, and T. G. Walker, Phys. Rev. A **86**, 033406 (2012).
[5] D. Maxwell, D. J. Szwer, D. Paredes-Barato, H. Busche, J. D. Pritchard, A. Gauguet, K. J. Weatherill, M. P. A. Jones, and C. S. Adams, Phys. Rev. Lett. **110**, 103001 (2013).
[6] R. C. Teixeira, C. Hermann-Avigliano, T. L. Nguyen, T. Cantat-Moltrecht, J. M. Raimond, S. Haroche, S. Gleyzes, and M. Brune, Phys. Rev. Lett. **115**, 013001 (2015).
[7] H. Park, P. J. Tanner, B. J. Claessens, E. S. Shuman, and T. F. Gallagher, Phys. Rev. A **84**, 022704 (2011).
[8] T. G. Walker and M. Saffman, Phys. Rev. A **77**, 032723 (2008).
[9] Y. Yu, H. Park, and T. F. Gallagher, Phys. Rev. Lett. **111**, 173001 (2013).
[10] K. A. Safinya, J. F. Delpech, F. Gounand, W. Sandner, and T. F. Gallagher, Phys. Rev. Lett. **47**, 405 (1981).
[11] I. Mourachko, D. Comparat, F. de Tomasi, A. Fioretti, P. Nosbaum, V. M. Akulin, and P. Pillet, Phys. Rev. Lett. **80**, 253 (1998).
[12] W. R. Anderson, J. R. Veale, and T. F. Gallagher, Phys. Rev. Lett. **80**, 249 (1998).
[13] B. Sun and F. Robicheaux, Phys. Rev. A **78**, 040701 (2008).
[14] I. Mourachko, W. Li, and T. F. Gallagher, Phys. Rev. A **70**, 031401 (2004).
[15] J. Han and T. F. Gallagher, Phys. Rev. A **79**, 053409 (2009).
[16] J. Han and T. F. Gallagher, Phys. Rev. A **77**, 015404 (2008).

[17] T. Amthor, M. Reetz-Lamour, S. Westermann, J. Denskat, and M. Weidemüller, Phys. Rev. Lett. **98**, 023004 (2007).